Numerical and experimental investigation of nonlinear ultrasonic Lamb waves at low frequency

Zuo, Peng; Zhou, Yu; Fan, Zheng

2016

https://hdl.handle.net/10356/81993

https://doi.org/10.1063/1.4958705

Numerical and experimental investigation of nonlinear ultrasonic Lamb waves at low frequency

Peng Zuo,[1] Yu Zhou,[2] and Zheng Fan[1,a)]

[1]*School of Mechanical and Aerospace Engineering, Nanyang Technological University, 50 Nanyang Avenue, Singapore 639798, Singapore*
[2]*Advanced Remanufacturing and Technology Center (ARTC), 3 Clean Tech Loop, CleanTech Two, Singapore 637143, Singapore*

Nonlinear ultrasonic Lamb waves are popular to characterize the nonlinearity of materials. However, the widely used nonlinear Lamb mode suffers from two associated complications: inherent dispersive and multimode natures. To overcome these, the symmetric Lamb mode (S0) at low frequency region is explored. At the low frequency region, the S0 mode is little dispersive and easy to generate. However, the secondary mode still exists, and increases linearly for significant distance. Numerical simulations and experiments are used to validate the nonlinear features and therefore demonstrate an easy alternative for nonlinear Lamb wave applications. *Published by AIP Publishing.*
[http://dx.doi.org/10.1063/1.4958705]

Nonlinear ultrasonic guided waves have emerged as a useful tool to characterize material microstructure and detect micro scale damages prior to the formation of macro-cracks in large structures, such as plates,[1–3] rods,[4,5] and pipe structures.[6,7] Comparing with nonlinear ultrasound in bulk media, nonlinear guided waves are much more complex in theory. Strict criteria have to be satisfied for the existence of nonlinear guided waves, including synchronism, i.e., the matching of phase velocities, as well as non-zero power flux from primary modes to the secondary modes.[1,8–10] Therefore nonlinear guided waves exist only in particular frequencies, and they appear in mode pairs. Theoretically there are an infinite number of mode pairs that satisfy the above conditions, although in the literature the mode pair (S1, S2) is most widely used, as it also has synchronous group velocities.[2,11–13] Fig. 1 presents the mode pair (S1, S2) at normalized frequencies $fd = 3.57$ and 7.14 MHz-mm on the phase velocity dispersion curves of an aluminum plate. In practice it may be difficult to generate the S1 mode at the exact resonant frequency, due to the uncertainty in the material properties used in the experiment. There are also challenges in the signal processing as multiple modes exist in that frequency and both S1 and S2 modes are dispersive. Although time frequency analysis, e.g., short time Fourier transformation (STFT), can be used to separate Lamb modes that are closely spaced, it suffers from the Heisenberg uncertainty principle, making it impossible to have perfect resolution in both time and frequency, and its resolutions depend strongly on the user's experience in determining the type and size of the window.[14] Because of these uncertainties, the post processing results for the time domain signal may be distorted.

In this paper, we explore the possibility to use low frequency symmetric Lamb mode (S0) for nonlinear applications. We will demonstrate that although the exact phase velocity matching criterion is no longer valid, the amplitude of the second harmonics still increases cumulatively for

significant distance. It has been reported that mismatch of the phase velocity, $c_p(2\omega) \neq c_p(\omega)$, where $c_p = \omega/k$ and k is the wavenumber, plus the nonzero power flux results in the sinusoidal behavior for the second harmonic wave.[8,15] Here $k_d = k(2\omega) - 2k(\omega)$ is interpreted as the deviation from exact phase velocity matching. In general, the sinusoidal behavior is not desired, since the amplitude of the second harmonic wave is bounded and oscillates with a spatial periodicity, called dispersion length L, given by a simple formula, $L = 2\pi/|k_d|$.[8] However, a special case would be practically useful: if k_d is very small, the sinusoidal solution for the second harmonic wave approaches closely to the resonant solution. In this case, the amplitude of the second harmonic wave grows almost linearly for a certain distance, which creates the possibility for practical applications. It can be seen from the dispersion curves that S0 mode is very little
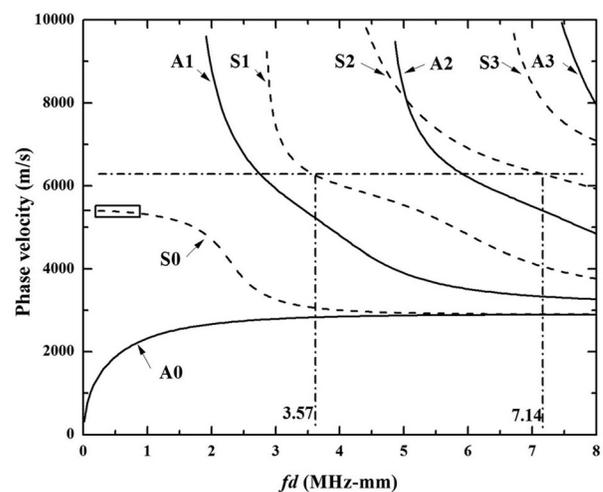

FIG. 1. Phase velocity dispersion curves for Lamb modes in aluminum plates. Symmetric modes (represented by S) are shown in dashed curves while antisymmetric modes (represented by A) are shown in solid curves. The box indicates the low frequency region and dotted dashed lines show the mode pair (S1, S2) satisfying the condition of the matching of phase velocity.

a)Electronic mail: ZFAN@ntu.edu.sg

dispersive in the low frequency region, leading to small k_d and thus cumulative increase of the second harmonics for a certain distance. This is interesting as the S0 mode is relatively easier to generate, and there are a wide range of frequencies that can be used. The objective of this paper was to explore the nonlinear feature of the low frequency region S0 mode via numerical simulations and experiments, and therefore demonstrate an easy alternative for nonlinear Lamb wave applications.

In the theoretical analysis, a perturbation approach and a mode expansion technique are used for the generation of second harmonic waves in nonlinear elastic plates.[1,8–10] The solutions for the primary wave can be obtained analytically via linear Lamb mode theory[16] or numerically via finite element (FE) modeling.[17] For the second harmonic wave, the modal expansion technique is employed for the inhomogeneous linear boundary value problem and the solution of the second harmonic wave is written as a linear combination of N propagating modes at the frequency of 2ω

$$\mathbf{v}^{(2)}(y, z, t) = \frac{1}{2}\sum_{n=1}^{N} A_n(z)\mathbf{v}_n^{(2)}(y)e^{-2I\omega t} + c.c., \qquad (1)$$

where z is the wave propagation direction and y represents the direction perpendicular to the plane of the plate; $\mathbf{v}_n^{(2)}(y)$ is the particle velocity of the n-th mode at 2ω; $c.c.$ represents the complex conjugates and $A_n(z)$ is the modal amplitude for the n-th mode in the expansion, which describes how strong a certain secondary mode is excited in the expansion. In this paper, the nonlinear Semi-Analytical Finite Element (SAFE) method was applied, which was developed to analyze the modal properties and nonlinear internal resonant conditions of arbitrary waveguides.[18,19]

An aluminum plate with thickness of 1 mm was considered in this study and the material properties are listed in Table I. The modal amplitude of the secondary modes with respect to the propagation distance was calculated through the nonlinear SAFE method with the S0 mode being the primary excitation. Fig. 2(a) plots the modal amplitudes of all possible secondary modes at a primary excitation frequency of 300 kHz. It is obvious that the modal amplitudes of both SH0 and A0 modes almost equal to zero along the propagation distance, which is due to zero power flux from the primary to the secondary modes. For the S0 mode, although it is not an internally resonant point, the modal amplitude increases almost linearly up to 500 mm (marked by an arrow in Fig. 2(a)) in the beginning part of its dispersion length of 2000 mm. From a practical application perspective, such distance is significant for applications of nonlinear Lamb waves. Fig. 2(b) plots the modal amplitudes of the propagative secondary modes with the S0 mode excitation at 600 kHz. In this situation, as the deviation between the phase velocity of the primary and second mode becomes larger, the
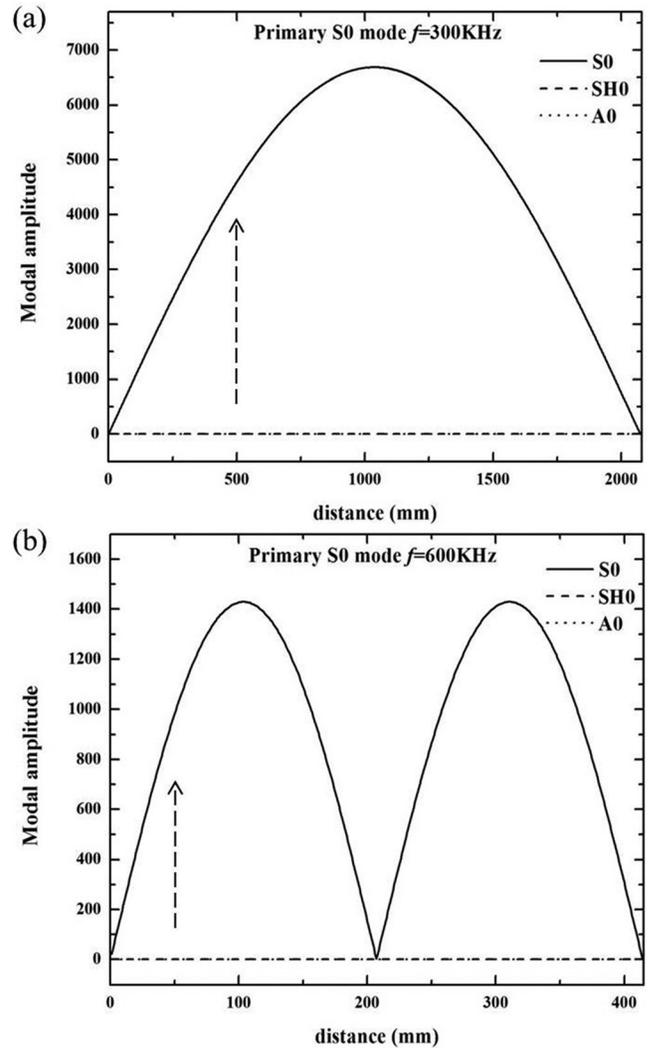

FIG. 2. Modal amplitudes for propagative secondary modes with excitation frequency of (a) 300 kHz and (b) 600 kHz. The arrows mark the distance where the amplitude of the secondary mode increases linearly; SH0 represents the zero order shear-horizontal mode.

dispersion length decreases to 200 mm, which results in a very short distance (50 mm, marked by an arrow in Fig. 2(b)) where the amplitude of the second harmonic wave grows linearly.

To validate the predictions from the nonlinear SAFE method, numerical simulations were carried out in a commercial finite element package.[20] The Murnaghan model was adopted in the simulations, which is equivalent to the Landau–Lifshitz nonlinear hyperelastic constitutive model in the nonlinear SAFE method[21] and plane strain condition was used. In simulations, the thickness of the plate was also chosen to be 1 mm and the length of the plate was assumed to be 600 mm. Prescribed displacement boundary condition as an input signal was applied at the left end of the plate to excite the primary mode, using a 10 cycle Hanning windowed toneburst with central frequencies of 300 kHz and 600 kHz, respectively. Stress free boundary conditions were applied to other boundaries. Rectangular elements were used with length of 0.2 mm and width of 0.1 mm, and a maximum time step of 0.01 μs was used. In addition, the monitor points were placed at the center of the plate to pick up the in-plane displacement at propagation distances in a step of 10 mm, as

TABLE I. Elastic constants used in numerical simulations.

ρ (kg/m^3)	λ (GPa)	μ (GPa)	A (GPa)	B (GPa)	C (GPa)
2700	55.27	25.95	-351.2	-149.4	-102.8

the maximum displacement occurs in the middle of the plate.[16] Fast Fourier Transform (FFT) was used in post-processing to extract the amplitudes of the primary mode (A_1) and the secondary mode (A_2). The relative nonlinearity parameter, A_2/A_1^2, was calculated as a function of the propagation distance to measure the nonlinearity.

Figure 3 shows the relative nonlinearity parameter with respect to the propagation distance. It can be observed that the numerical results agree very well with the predictions from the nonlinear SAFE method. Fig. 3(a), with the primary S0 mode excited at 300 kHz, demonstrates that the amplitude of the secondary mode increases linearly with the propagation distance at least from 10 to 500 mm. In Fig. 3(b), when the excitation frequency is 600 kHz, the relative nonlinearity parameter captures the sinusoidal behavior, and the linear cumulative increase of the secondary mode is prominent at the beginning distance of each dispersion length, e.g., 0–50 mm and 200–250 mm.

In addition to numerical simulation validations, experiments were designed to verify the nonlinear feature of the low frequency region S0 mode on a 1 mm thick aluminum plate (Al 1100). Two wide-band piezoelectric shear wave transducers (manufactured by Doppler Electronic Technologies

Co.) with central frequency of 300 kHz and 600 kHz, respectively, and diameter of 30 mm were placed on the top surface of the plate to excite the primary S0 mode. A high voltage 10 cycle Hanning windowed tone-burst signal was generated by a high power gated amplifier (RITEC RAM-5000 SNAP). The ultrasonic waves were measured using two laser vibrometers (Polytec OFV 5000) to pick up the in-plane displacement of a point on the plate surface along the wave propagation direction. An oscilloscope was used to store the time trace of the signal with 1000 averages to improve the signal-to-noise ratio and the data were processed in the frequency domain using FFT. In each experiment, measurements were made in the far field along the propagation distances, from 90 to 390 mm with a step of 30 mm, and each set of measurements was repeated five times.

Figure 4 shows the relative nonlinearity parameter with the propagation distance with excitation frequency of 300 kHz and 600 kHz, respectively. In the first case, when the excitation frequency is 300 kHz, the linear rise of the relative nonlinearity parameter with increasing propagation is clearly shown from 90 to 390 mm in Fig. 4(a), which demonstrates a cumulative second harmonic generation in this distance. When the excitation frequency is 600 kHz, a sinusoidal type
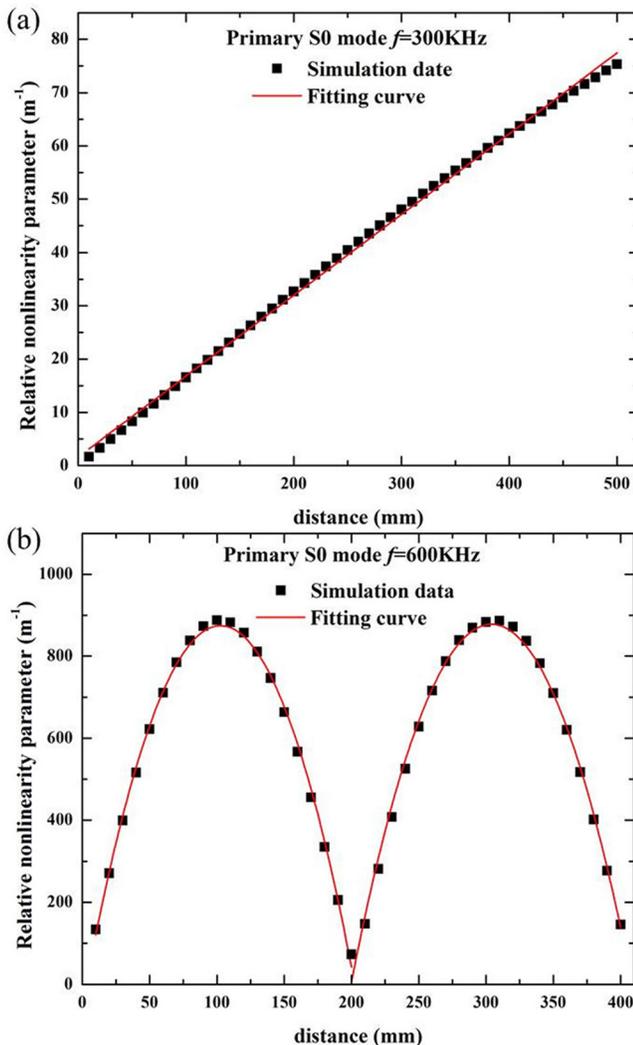

FIG. 3. Relative nonlinearity parameter with respect to the propagation distance with excitation frequency of (a) 300 kHz and (b) 600 kHz.
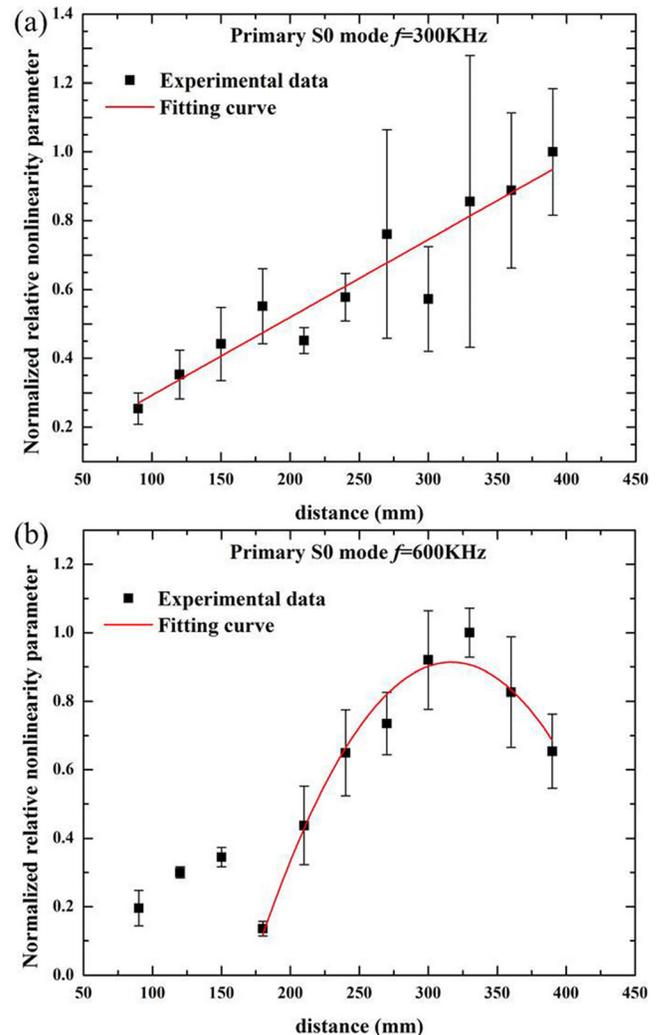

FIG. 4. Relative nonlinearity parameter measured over increasing propagation distance for the aluminum plate with excitation frequency of (a) 300 kHz and (b) 600 kHz.
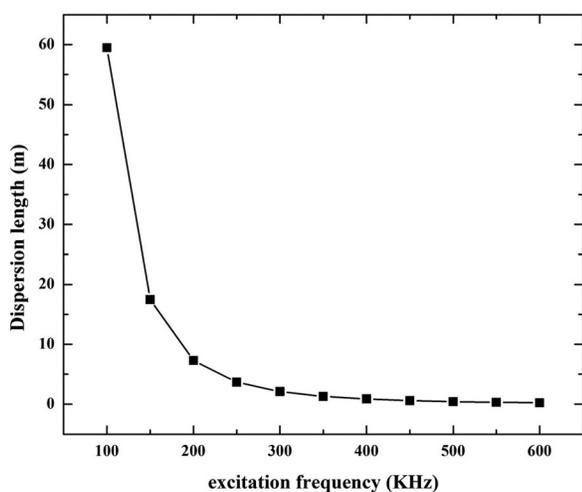
FIG. 5. Dispersion length with respect to excitation frequencies for the low frequency S0 wave (calculated for a 1 mm thick plate by the dispersion length formula).

of curve is shown in Fig. 4(b) between 200 and 400 mm, which means that the amplitude of the secondary mode increases first and then decreases with a sinusoidal behavior in the distance. It should be noted that the first sinusoidal curve between 0 and 200 mm is not easy to be captured experimentally mainly due to the near field effect. Such results have very close agreement with the predictions from the nonlinear SAFE calculation and the numerical simulations, indicating that the amplitude of the second harmonic wave indeed grows linearly in a certain distance at the low frequency region.

It has been known that large dispersion length can be obtained for lower frequency, thus leading to a long distance along which the second harmonic wave grows linearly (shown in Fig. 5). However, it should be noted that the non-linear parameter,[22] $\beta = 8A_2/k^2 x A_1^2$, is a material property dependent only on the microstructure. Therefore the amplitude of the second harmonic (A_2) is proportional to the square of the amplitude of the primary wave (A_1). At very low frequency, where the wavenumber k is small, A_1 needs to be very high to generate noticeable signal of the second harmonics, which is practically difficult in experiments. Therefore, the selection of the excitation frequency of the S0 mode needs to be a compromise between the dispersion length and the experimental complexity. On the other side, a quick way for selections of excitation frequencies in experiments for the

low frequency S0 mode can be established. It can be assumed that the second harmonic wave increases almost linearly in the first quarter (25%) of the sinusoidal dispersion length. Therefore, for a given inspection length, the frequency range can be selected according to Fig. 5.

In this paper, the low frequency S0 mode is demonstrated as an alternative for nonlinear Lamb wave applications. This mode is little dispersive and easy to generate, and the second harmonic wave grows linearly along a significant distance. Numerical simulations and experiments have been carried out to validate these features. The excitation frequency can be selected by the computation of the dispersion length as well as practical concerns in the experiments.

[1]M. X. Deng, J. Appl. Phys. **94**, 4152 (2003).
[2]C. Bermes, J. Y. Kim, J. M. Qu, and L. J. Jacobs, Appl. Phys. Lett. **90**, 021901 (2007).
[3]Y. Liu, V. K. Chillara, C. J. Lissenden, and J. L. Rose, J. Appl. Phys. **114**, 114908 (2013).
[4]W. J. N. de Lima and M. F. Hamilton, Wave Motion **41**, 1 (2005).
[5]A. Srivastava and F. L. di Scalea, J. Sound Vib. **329**, 1499 (2010).
[6]Y. Liu, C. J. Lissenden, and J. L. Rose, J. Appl. Phys. **115**, 214901 (2014).
[7]Y. Liu, C. J. Lissenden, and J. L. Rose, J. Appl. Phys. **115**, 214902 (2014).
[8]W. J. N. de Lima and M. F. Hamilton, J. Sound Vib. **265**, 819 (2003).
[9]A. Srivastava and F. L. di Scalea, J. Sound Vib. **323**, 932 (2009).
[10]M. F. Müller, J. Y. Kim, J. M. Qu, and L. J. Jacobs, J. Acoust. Soc. Am. **127**, 2141 (2010).
[11]N. Matsuda and S. Biwa, J. Appl. Phys. **109**, 094903 (2011).
[12]C. Pruell, J. Y. Kim, J. M. Qu, and L. J. Jacobs, Appl. Phys. Lett. **91**, 231911 (2007).
[13]C. Pruell, J. Y. Kim, J. M. Qu, and L. J. Jacobs, Smart Mater. Struct. **18**, 035003 (2009).
[14]M. Niethammer, L. J. Jacobs, J. Qu, and J. Jarzynski, J. Acoust. Soc. Am. **109**, 1841 (2001).
[15]Y. X. Xiang, M. X. Deng, and F. Z. Xuan, J. Appl. Phys. **106**, 024902 (2009).
[16]K. F. Graff, *Wave Motion in Elastic Solids* (Courier Corporation, 2012).
[17]L. Gavrić, J. Sound Vib. **185**, 531 (1995).
[18]C. Nucera and F. L. di Scalea, J. Eng. Mech. **140**, 502 (2014).
[19]C. Nucera and F. L. di Scalea, J. Acoust. Soc. Am. **136**, 2561 (2014).
[20]COMSOL, See http://www.comsol.com/ for User's Guide and Introduction, version 4.4, COMSOL MULTIPHYSICS; accessed 20 December 2015.
[21]V. K. Chillara and C. J. Lissenden, Opt. Eng. **55**, 011002 (2015).
[22]K. H. Matlack, J. Y. Kim, L. J. Jacobs, and J. M. Qu, "Review of second harmonic generation measurement techniques for material state determination in metals," J. Nondestr. Eval. **34**, 273 (2015).